

# Late-Time Evolution of Charged Gravitational Collapse and Decay of Charged Scalar Hair - III. Nonlinear Analysis

Shahar Hod and Tsvi Piran

*The Racah Institute for Physics, The Hebrew University, Jerusalem 91904, Israel*

(November 26, 2024)

## Abstract

We study the *nonlinear* gravitational collapse of a *charged* massless scalar-field. We confirm the existence of oscillatory inverse power-law tails along future timelike infinity, future null infinity and along the future outer-horizon. The *nonlinear* dumping exponents are in excellent agreement with the *analytically* predicted ones. Our results prove the analytic conjecture according to which a *charged* hair decays *slower* than a neutral one and also suggest the occurrence of mass-inflation along the Cauchy horizon of a *dynamically* formed charged black-hole.

## I. INTRODUCTION

Linearized *perturbation* analysis have revealed important dynamical features of the gravitational collapse of massless neutral fields. In particular, according to the linearized perturbation theory there are two major features which characterize the *late* stages of the evolution: quasinormal ringing and inverse power-law tails (which follows the quasinormal ringing). These late-time tails are relevant to two major aspects of black-hole physics: The *no-hair theorem* of Wheeler and the *mass-inflation* scenario [1]. The mechanism responsible for the development of these neutral inverse power-law tails was first studied by Price [2]. This work was further extended by Gundlach, Price and Pullin [3]. These authors have

also shown that the nonlinear dumping exponents, describing the fall-off of a massless neutral scalar-field at late-times, are in good agreement with the prediction of the linearized perturbation analysis [4].

The late-time evolution of a *charged* massless scalar-field and the physical mechanism for the radiation of a *charged* hair were first studied *analytically* in [5,6], hereafter referred to as papers I and II, respectively. The main result presented there is the existence of oscillatory inverse power-law tails along the asymptotic regions of future timelike infinity, future null infinity and along the future outer-horizon with *smaller* (compared to the neutral case) dumping exponents. These dumping exponents depend on the black-hole's (or the star's) charge. In this paper we study numerically the fully *nonlinear* gravitational collapse of a massless *charged* scalar-field. We confirm that the late-time behaviour of the fully *nonlinear* evolution is in excellent agreement with the *analytical* predictions of the linearized analysis.

The plan of the paper is as follows. In Sec. II we give a short review of the linearized *analytical* results of papers I and II, on which we base our expectations for the fully nonlinear case. In Sec. III we describe our physical system, namely the coupled Einstein-Maxwell-charged scalar equations. In Sec. IV we study the late-time evolution of the *nonlinear* spherical charged gravitational collapse. In Sec. V we study the late-time evolution of non-spherical perturbations on a fixed Reissner-Nordström background and on a time-dependent background. In all cases we compare the *nonlinear* results with the predictions of the linearized *analytical* theory. We conclude in Sec. VI with a brief summary of our results and their physical implications.

## II. REVIEW OF LINEARIZED ANALYTICAL RESULTS

We study numerically the late-time behaviour of the fully *nonlinear* gravitational collapse of a massless *charged* scalar-field. Our expectations are based on the *linearized analytical* results of papers I and II. Due to the *smallness* of the field's amplitude at late times, we expect these results to hold even in the fully *nonlinear* case. In other words, we expect

that the late-time field may be regarded as a small perturbation. Thus, our expectations include the existence of inverse *power-law* tails along the three asymptotic regions: timelike infinity  $i_+$ , future null infinity  $scri_+$  and along the black-hole outer-horizon  $H_+$  (where the power-law is multiplied by a *periodic* term). Quantitatively, in paper II it was found that the *late-time* behaviour of linearized *charged-scalar* perturbations (on a Reissner-Nordström background) is dominated by power-law tails of the form

$$\psi_m^l = A_{ti}(l, eQ) y^{\beta+1} t^{-(2\beta+2)} , \quad (1)$$

at timelike infinity  $i_+$ ,

$$\psi_m^l = A_{ni}(l, eQ) v_e^{-ieQ} u_e^{-(\beta+1-ieQ)} , \quad (2)$$

at future null infinity  $scri_+$  and

$$\psi_m^l = A_{ch}(l, eQ) e^{i\frac{eQ}{r_+}y} v_e^{-(2\beta+2)} , \quad (3)$$

along the black-hole outer-horizon  $H_+$ , where the charged scalar-field  $\phi$  is given by

$$\phi = e^{ie\Phi t} \sum_{l,m} \psi_m^l(t, r) Y_l^m(\theta, \varphi) / r , \quad (4)$$

where  $\Phi$  is merely a gauge constant of the electromagnetic potential  $A_t$ , i.e. its value at infinity ( $A_t$  is given by  $A_t = \Phi - \frac{Q}{r}$ ). The constant  $\beta(l, eQ)$  is given by

$$\beta = \frac{-1 + \sqrt{(2l+1)^2 - 4(eQ)^2}}{2} . \quad (5)$$

The tortoise radial coordinate  $y$  is defined by  $dy = dr/\lambda^2$ , where  $\lambda^2 = 1 - \frac{2M}{r} + \frac{Q^2}{r^2}$ . Here  $v_e \equiv t+y$  and  $u_e \equiv t-y$  are the ingoing and outgoing Eddington-Finkelstein null coordinates, respectively. The expressions for the coefficients  $A(l, eQ)$  are given in paper II.

### III. THE EINSTEIN-MAXWELL-CHARGED SCALAR EQUATIONS

We consider a spherically-symmetric self-gravitating *charged* scalar-field  $\phi$ . The system is described by the coupled Einstein-Maxwell-charged scalar equations. This physical system

was already described in a previous paper [7]. Here we give only a short description of the system and the final form of the equations studied. We express the metric of a spherically symmetric spacetime in the form [8,9]

$$ds^2 = -g(u, r)\bar{g}(u, r)du^2 - 2g(u, r)dudr + r^2d\Omega^2 , \quad (6)$$

in which  $u$  is a retarded time null coordinate and the radial coordinate  $r$  is a geometric quantity which directly measures surface area. The coordinates have been normalized so that  $u$  is the proper time on the  $r = 0$  central world line. We use the auxiliary field  $\tilde{\phi}$  defined by

$$\phi \equiv \frac{1}{r} \int_0^r \tilde{\phi} dr , \quad (7)$$

in terms of which the Einstein equations yield

$$g(u, r) = \exp \left[ 4\pi \int_0^r \frac{(\tilde{\phi} - \phi)(\tilde{\phi}^* - \phi^*)}{r} dr \right] , \quad (8)$$

and

$$\bar{g}(u, r) = \frac{1}{r} \int_0^r \left( 1 - \frac{Q^2}{r^2} \right) g dr . \quad (9)$$

The electromagnetic potential  $A_u$  is given by the Maxwell equations

$$A_u = \int_0^r \frac{Q}{r^2} g dr , \quad (10)$$

where the charge  $Q(u, r)$  within a sphere of radius  $r$ , at a retarded time  $u$  is given by

$$Q(u, r) = 4\pi ie \int_0^r r(\phi^* \tilde{\phi} - \phi \tilde{\phi}^*) dr . \quad (11)$$

The mass  $M(u, r)$  within a sphere of radius  $r$ , at a retarded time  $u$  is given by

$$M(u, r) = \int_0^r \left[ 2\pi \frac{\bar{g}}{g} (\tilde{\phi} - \phi)(\tilde{\phi}^* - \phi^*) + \frac{1}{2} \frac{Q^2}{r^2} \right] dr + \frac{1}{2} \frac{Q^2}{r} . \quad (12)$$

Finally, the wave-equation for the charged scalar-field takes the form of a pair of coupled differential equations

$$\frac{d\tilde{\phi}}{du} = \frac{1}{2r}(g - \bar{g})(\tilde{\phi} - \phi) - \frac{Q^2}{2r^3}(\tilde{\phi} - \phi)g - \frac{ieQ}{2r}g\phi - ie\tilde{\phi}A_u, \quad (13)$$

and

$$\frac{dr}{du} = -\frac{1}{2}\bar{g}. \quad (14)$$

We solve this system of equations numerically. A detailed description of our algorithm, numerical methods, discretization and error analysis are given in Ref. [7].

In order to compare our *nonlinear* results with the linearized *analytical* results of papers I and II, we use another spacetime coordinate, namely the Bondi time  $t_B \equiv t(u, \infty)$ , which is the retarded time coordinate that agrees with time at infinity. The proper time  $t(u, r)$  along an  $r = \text{const}$  trajectory is given by [4]

$$t(u, r) \equiv \int_0^u \sqrt{g(u', r)\bar{g}(u', r)} du'. \quad (15)$$

The comparison with the analytical results also requires the usage of the ingoing and outgoing Eddington-Finkelstein null coordinates  $v_e$  and  $u_e$ . In the asymptotic region  $r \gg M_{BH}$ ,  $v_e$  is linear with  $r$  (along a  $u = \text{const}$  ray). In particular,  $v_e \simeq 2y \simeq 2r$  along the  $u = u_e = 0$  ray. In a similar way  $u_e$  is linear with  $t$  along a  $v = \text{const}$  ray, namely  $u_e = 2t - v_e$  (one may also use the asymptotic relation  $u_e \simeq v_e - 2r$  along a  $v = \text{const}$  ray in order to evaluate  $u_e$ ). The relation between  $A_u$  and  $A_t$  implies that  $A_t(r_+) = 0$ , i.e.  $\Phi = \frac{Q}{r_+}$ .

#### IV. NONLINEAR SPHERICAL COLLAPSE

In this section we present our results for the *nonlinear* spherically symmetric gravitational collapse of the self-gravitating massless *charged* scalar-field. We have focused our attention on the behaviour of the charged field  $\phi$  along the three asymptotic regions: timelike infinity  $i_+$ , null infinity  $scri_+$  and the black-hole outer horizon  $H_+$ . The late-time evolution of a charged scalar-field is independent of the form of the initial data. The numerical results presented here have an initial profile of the form

$$\phi(u = 0, r) = Ar^2 \exp \left\{ -[(r - r_0)/\sigma]^2 \right\} , \quad (16)$$

where  $r_0 = 2.5, \sigma = 0.5$  for the real part of the complex field and  $r_0 = 3.0, \sigma = 0.5$  for the imaginary part. Figure 1 displays the time evolution of  $\phi_R$ , the real part of the charged scalar-field, along these asymptotic regions for a *supercritical* evolution ( $A = 0.005, e = 0.85$ ) in which a black-hole forms. The mass and charge of the formed black-hole are  $M_{BH} = 0.503$  and  $Q_{BH} = -0.420$ , respectively. The top panel shows the behaviour of the field at a constant radius (here  $r = 10$ ) as a function of the Bondi time. The middle panel shows the behaviour of the field along null infinity (approximated by the null surface  $v = v_{max}$ , where  $v_{max}$  is the largest value of  $v$  on the grid) as a function of  $u_e$ . The bottom panel shows the behaviour of the field along the black-hole outer horizon  $H_+$  (approximated by the null surface  $u = u_{max}$ , where  $u_{max}$  is the largest value of  $u$  on the grid) as a function of  $v_e$ . Initially, the evolution is dominated by the prompt contribution and by the quasinormal ringing. However, at late-times a definite oscillatory *power-law* fall off is manifest. The *nonlinear* power-law exponents (determined from the maximas of these oscillations) are  $-1.78$  at time-like infinity,  $-0.86$  along null infinity and  $-1.96$  along the black-hole outer horizon. These values should be compared with the *analytically* predicted values of  $-1.70, -0.85, -1.70$ , [see Eqs. (1) – (3)], respectively. The theoretical values of the oscillation frequencies of the charged scalar field  $\phi$  are  $\frac{eQ_{BH}}{r_+}$  at timelike infinity and along the black-hole outer horizon and  $\frac{eQ_{BH}}{2r_+}$  along null infinity [see Eq. (4) and the relation  $\Phi = \frac{Q}{r_+}$ ]. These values agree to within 2% with the numerical estimates.

While the dumping exponents and the decay-rate of neutral perturbations are independent of the spacetime parameters ( $M$  and  $Q$ ), the analysis of paper II predicts that the *charged* dumping exponents depend on the black-hole's (or the star's) *charge* (namely, on the dimensionless quantity  $|eQ|$ ). In order to test this linearized *analytical* prediction, we have studied the dependence of the charged dumping exponents at timelike infinity on the parameter  $e$ . The initial form of the field is given by (16) and the amplitude is set to  $A = 0.005$ . The nonlinear results are summarized in table I. We find a good agreement

between the numerically measured exponents and the linearized predicted ones.

The analysis of paper I predicts the existence of charged power-law tails even in subcritical evolution when there is no collapse to a black-hole (and all we have are imploding and exploding shells). This phenomena is related to the fact that the late-time evolution of the field is dominated by the backscattering from asymptotically *far* regions, and it does *not* depend on the small- $r$  details of the spacetime (this is also the situation for neutral massless perturbations [3]). Since the charge of the spacetime is a *dynamical* quantity it is not clear which value of  $Q$  should be taken in calculating the value of the dumping exponent. However, since the charge of the spacetime falls to zero asymptotically we expect the effective value of  $|eQ|$  to be much *smaller* than unity. In this case the dumping exponents are expected to be  $2l + 2$  at timelike infinity and  $l + 1$  along null infinity (with small corrections of order  $O[(eQ)^2]$ ). Figure 2 displays the time evolution of  $\phi_R$  for a *subcritical* evolution ( $A=0.002$ ,  $e=3$ ). Shown are the behaviour of the field at a constant radius (here  $r = 10$ ) as a function of Bondi time and along null infinity as a function of  $u_e$ . The *nonlinear* power-law exponents are  $-2.00$  at timelike infinity and  $-1.00$  along null infinity. These values are exactly equal to those predicted in paper I.

## V. NON-SPHERICAL PERTURBATIONS OF SPHERICAL COLLAPSE

In order to study the dependence of the late-time dumping-exponents on the multipole index  $l$  we have performed two series of numerical investigations. First, we have integrated the *linearized charged* scalar-field equation

$$\psi_{,tt} + 2ie\frac{Q}{r}\psi_{,t} - \psi_{,yy} + V\psi = 0, \quad (17)$$

where

$$V = V_{M,Q,l,e}(r) = \left(1 - \frac{2M}{r} + \frac{Q^2}{r^2}\right) \left[\frac{l(l+1)}{r^2} + \frac{2M}{r^3} - \frac{2Q^2}{r^4}\right] - e^2\frac{Q^2}{r^2}, \quad (18)$$

on a *fixed* Reissner-Nordström background. It is straightforward to integrate Eq. (17) using the method described in [3]. The late-time evolution of a charged scalar-field is independent

of the form of the initial data. The results presented here are of a Gaussian pulse on  $u = 0$

$$\psi(u = 0, v) = A \exp \left\{ - \left[ (v - v_0) / \sigma \right]^2 \right\} , \quad (19)$$

where the amplitude  $A$  is physically irrelevant due to the linearity of Eq. (17). It should be noted that the evolution equation (17) is invariant under the rescaling

$$r \rightarrow ar , \quad t \rightarrow at , \quad M \rightarrow aM , \quad Q \rightarrow aQ , \quad e \rightarrow e/a , \quad (20)$$

where  $a$  is some positive constant. The black-hole mass and charge are set equal to  $M_{BH} = 0.5$  and  $Q_{BH} = 0.45$ , respectively. We have chosen  $e = 0.01$ ,  $v_0 = 100$  and  $\sigma = 20$  (for both the real and the imaginary parts of the charged field). The numerical results for the  $l=0,1$  and 2 modes are shown in Fig. 3. (from top to bottom, respectively). This figure demonstrates the dependence of the late-time tails at  $i_+$  (here  $y=400$ ) on the multipole index  $l$ . A definite *power-law* fall off is manifest at late-times. The numerical values of the power-law exponents, describing the fall-off of the field at *late* times are  $-1.97$ ,  $-3.94$  and  $-5.75$  for  $l=0,1$  and 2, respectively. These values are to be compared with the *analytically* predicted values of  $-2.0$ ,  $-4.0$  and  $-6.0$ , respectively.

In a second series of numerical investigation, we have studied the evolution of a second perturbative charged scalar-field  $\xi$  evolved on a *time-dependent* spacetime. This time-dependent spacetime is determined by the background solution  $\phi$ , while we ignore the contribution of the field  $\xi$  to the energy-momentum tensor (this is analogous to the case studied in [4] for a neutral field). Resolving the field into spherical harmonics  $\xi = \sum_{l,m} \xi_m^l(t, r) Y_l^m(\theta, \varphi)$  (and using the spherical symmetry of the time-dependent background) one obtains a wave-equation for each multiple moment of the field  $\xi$

$$\frac{d\tilde{\xi}_m^l}{du} = \frac{1}{2r}(g - \bar{g})(\tilde{\xi}_m^l - \xi_m^l) - \frac{Q^2}{2r^3}(\tilde{\xi}_m^l - \xi_m^l)g - \frac{ieQ}{2r}g\xi_m^l - ie\tilde{\xi}_m^l A_u - \frac{1}{2r}l(l+1)g\xi_m^l , \quad (21)$$

[together with Eq. (14)], where

$$\xi_m^l \equiv \frac{1}{r} \int_0^r \tilde{\xi}_m^l dr . \quad (22)$$



The quantities  $g, \bar{g}$  and  $Q$  are still determined by the background solution for the field  $\phi$ . For the background field  $\phi$  we choose the same initial form as in Sec. IV. The most interesting time-dependent backgrounds are the *non-collapsing* ones. Thus, we take the *subcritical* initial conditions  $A=0.002$  and  $e=3$  of Sec. IV. For the perturbation field  $\xi$  we choose initial data of the form Eq. (16) with  $r_0 = 4.0$  and  $\sigma = 0.5$  for both the real and the imaginary parts of the field (again, the amplitude of the perturbation field is physically irrelevant). Figure 4 displays the time evolution of the perturbative charged scalar field  $\xi$  (its real part) at a constant radius (here  $r = 10$ ) as a function of Bondi time. It is interesting that even for *time-dependent* spacetimes the late-time behaviour of charged-fields is well described by an inverse *power-law* fall-off. The numerical values of the power-law exponents are  $-1.99$  for the  $l=0$  mode (top panel) and  $-4.16$  for the  $l=1$  mode (bottom panel). These values should be compared with the fixed background *analytically* predicted values of  $-2.0$  and  $-4.0$ , respectively.

## VI. SUMMARY AND PHYSICAL IMPLICATIONS

We have studied the *nonlinear* gravitational collapse of a massless *charged* scalar-field. Following the predictions of the linearized *analytical* theory (papers I and II) we have focused attention on the *asymptotic* late-time evolution of the charged-field. Our main results and their physical implications are:

We have confirmed the existence of oscillatory inverse *power-law tails* in a *collapsing* spacetime along the asymptotic regions of future timelike infinity  $i_+$ , future null infinity  $scri_+$  and along the future outer-horizon  $H_+$ . The *nonlinear* dumping exponents are in excellent agreement with the *analytically* predicted ones. In particular, we have verified the analytically conjectured dependence of the *charged* dumping exponents on the dimensionless quantity  $|eQ|$ . This dependence on the spacetime charge is contrasted to neutral perturbations, where the dumping exponents are fixed integers which does *not* depend on the spacetime parameters (namely, they are functions of the multipole index  $l$  only). We have

confirmed the existence of power-law tails even in non-collapsing spacetimes (i.e. imploding and exploding shells).

We have also studied the late-time evolution of non-spherical perturbations (*charged* test fields) on a fixed Reissner-Nordström background and on a time-dependent background. In both cases we have found that the dumping exponents, describing the fall-off of the charged field at late-times, are in good agreement with the predictions of the linearized analytical theory (In particular, we have verified the functional dependence of the dumping exponents on the multipole index  $l$ ).

Our nonlinear results verify the analytic conjecture that a *charged* hair decays *slower* than a neutral one. Furthermore, the existence of oscillatory inverse *power-law* tails along the black-hole outer horizon suggests the occurrence of the well-known phenomena of *mass-inflation* [1] along the Cauchy horizon of a *dynamically* formed charged black-hole.

In a forthcoming paper we study the *fully nonlinear* gravitational collapse of a charged scalar-field, using a different numerical scheme which is based on *double* null coordinates. This scheme allows us to start with *regular* initial conditions (at approximately past null infinity), calculating the *formation* of the regular black-hole's event horizon, and continue the evolution all the way *inside* the black-hole. Thus, this numerical scheme makes it possible to test the mass-inflation conjecture during the gravitational collapse of a *charged* scalar-field. To our knowledge, the mass-inflation scenario has *never* been demonstrated explicitly before in *collapsing* situations (The numerical work of Brady and Smith [10] begins on a Reissner-Nordström spacetime and the black-hole formation itself was *not* calculated there).

## ACKNOWLEDGMENTS

This research was supported by a grant from the Israel Science Foundation.

## REFERENCES

- [1] E. Poisson and W. Israel, Phys. Rev. **D41**, 1796 (1990).
- [2] R.H. Price, Phys. Rev. **D5**, 2419 (1972).
- [3] C. Gundlach, R.H. Price, and J. Pullin, Phys. Rev. **D49**, 883 (1994).
- [4] C. Gundlach, R.H. Price, and J. Pullin, Phys. Rev. **D49**, 890 (1994).
- [5] S. Hod and T. Piran, gr-qc/9712041, Submitted to Phys. Rev. **D**.
- [6] S. Hod and T. Piran, gr-qc/9801001, Submitted to Phys. Rev. **D**.
- [7] S. Hod and T. Piran, Phys. Rev. **D55**, 3485 (1997).
- [8] D. Christodoulou, Commun. Math. Phys. **105**, 337 (1986).
- [9] D. S. Goldwirth and T. Piran, Phys. Rev. **D36**, 3575 (1987).
- [10] P. R. Brady and J. D. Smith, Phys. Rev. Lett. **75**, 1256 (1995).

## FIGURES

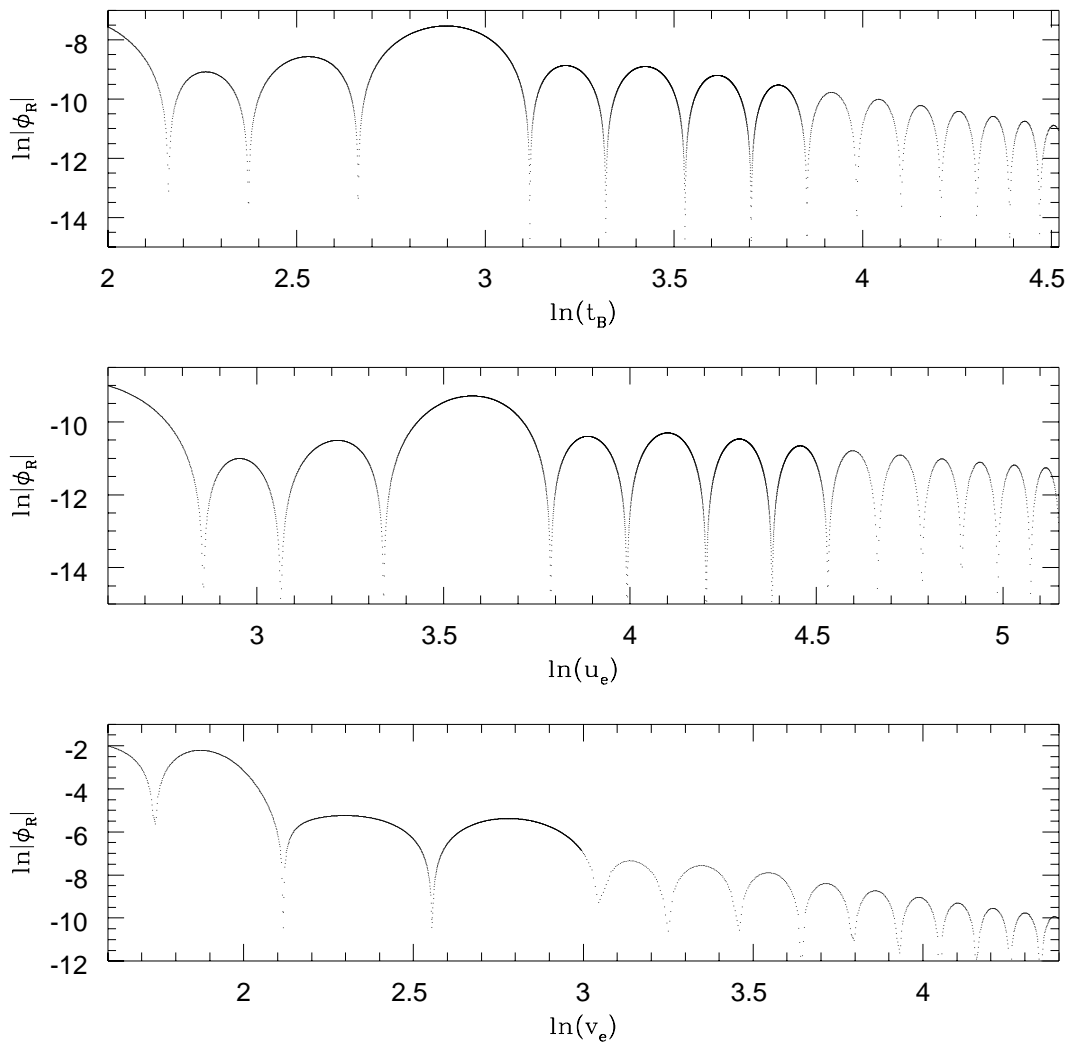


FIG. 1. Supercritical evolution of the charged field  $|\phi_R|$  along the asymptotic regions of time-like infinity (top panel), null infinity (middle panel) and the black-hole outer horizon (bottom panel). The initial data is a Gaussian distribution (multiplied by an  $r^2$  factor). The field's amplitude is  $A=0.005$  and  $e=0.85$ . The mass and charge of the formed black-hole are  $M_{BH} = 0.503$  and  $Q_{BH} = -0.420$ , respectively. A definite oscillatory *power-law* fall-off is manifest at late-times. The *nonlinear* power-law exponents are  $-1.78$  at timelike infinity (here  $r = 10$ ),  $-0.86$  along null infinity and  $-1.96$  along the black-hole outer horizon. These values are to be compared with the *analytically* predicted values of  $-1.70$ ,  $-0.85$  and  $-1.70$ , respectively. The oscillation frequency of the charged field  $\phi$  agrees with the *analytically* predicted value to within 2%.

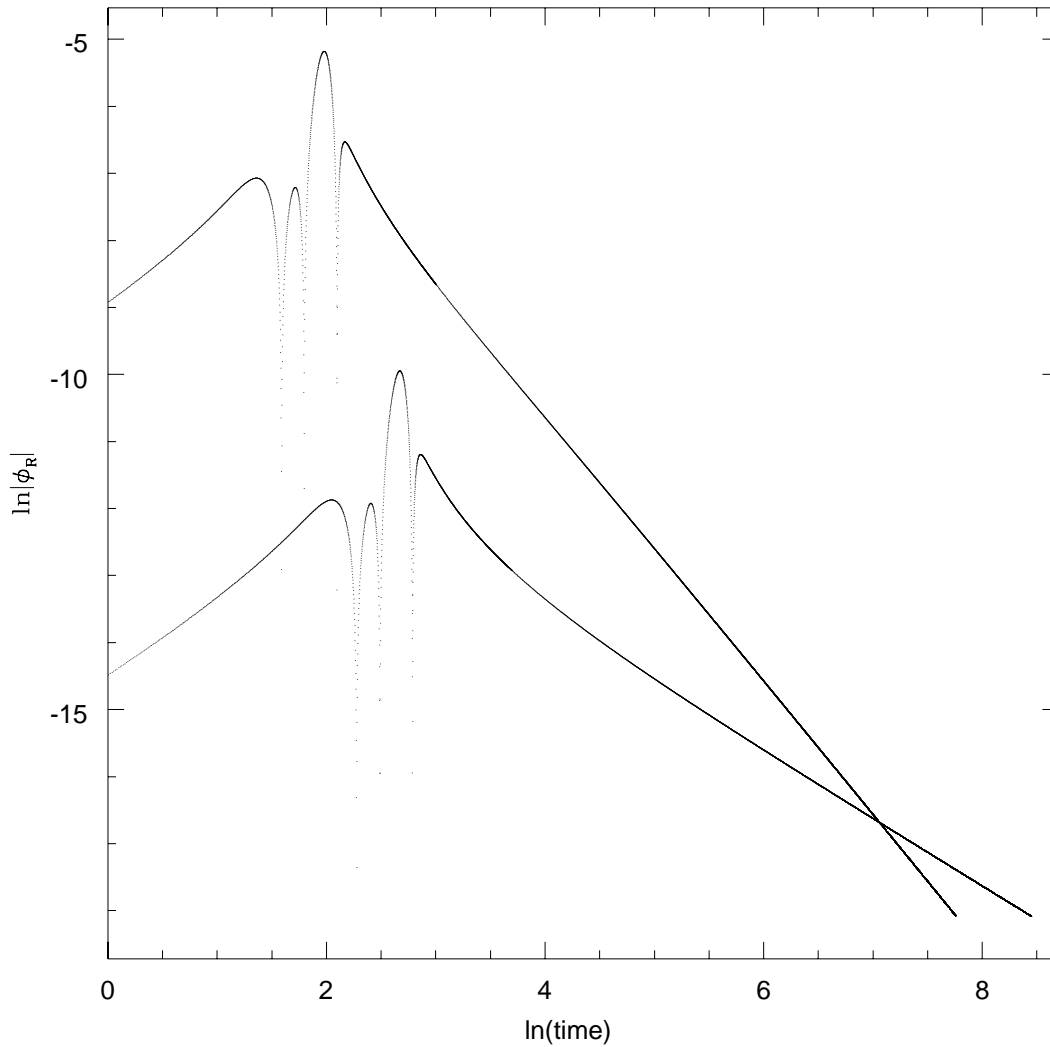


FIG. 2. Subcritical evolution of the charged field  $|\phi_R|$ . The initial form of the field is the same as in Fig. 1. The field's amplitude is  $A=0.002$  and  $e=3$ . The field at future timelike infinity ( $r = 10$ ) is shown as a function of  $t_B$ . Along null infinity the field is shown as a function of  $u_e$ . A definite *power-law* fall-off is manifest at late-times. The *nonlinear* power-law exponents are  $-2.00$  at timelike infinity and  $-1.00$  along null infinity. These values are exactly the ones predicted by the linearized *analytical* approach.

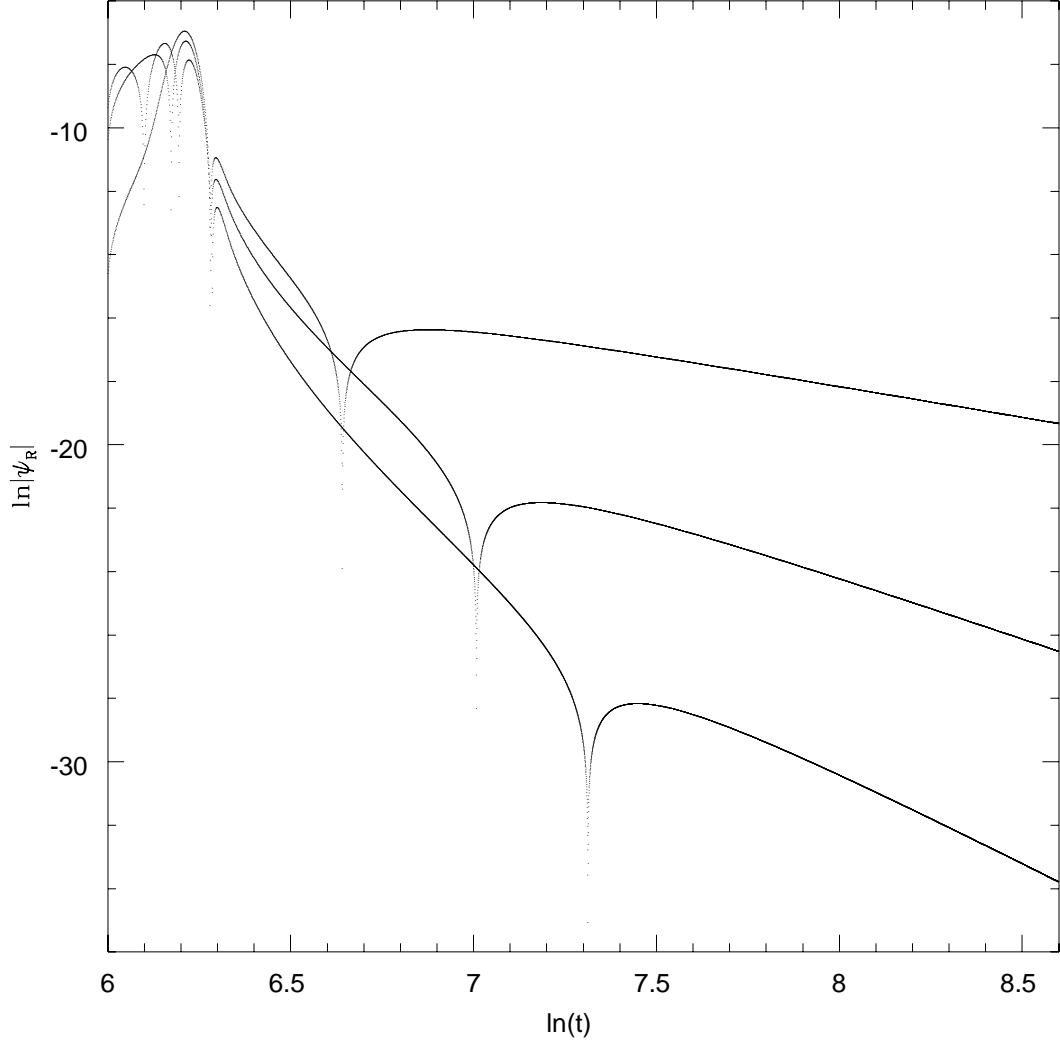


FIG. 3. Evolution of the charged field  $|\psi_R(y = 400, t)|$  on a fixed Reissner-Nordström background for different multipoles  $l=0,1$  and  $2$  (from top to bottom, respectively). The black-hole mass and charge are set equal to  $M_{BH} = 0.5$  and  $Q_{BH} = 0.45$ , respectively. The field's charge is  $e = 0.01$ . The initial data is a Gaussian distribution with  $v_0 = 100$  and  $\sigma = 20$  (for both the real and the imaginary parts of the field). A definite *power-law* fall-off is manifest at late-times. The power-law exponents are  $-1.97, -3.94$  and  $-5.75$  for the  $l=0,1$  and  $2$  modes, respectively. These values are to be compared with the *analytically* predicted values of  $-2.0, -4.0$  and  $-6.0$ .

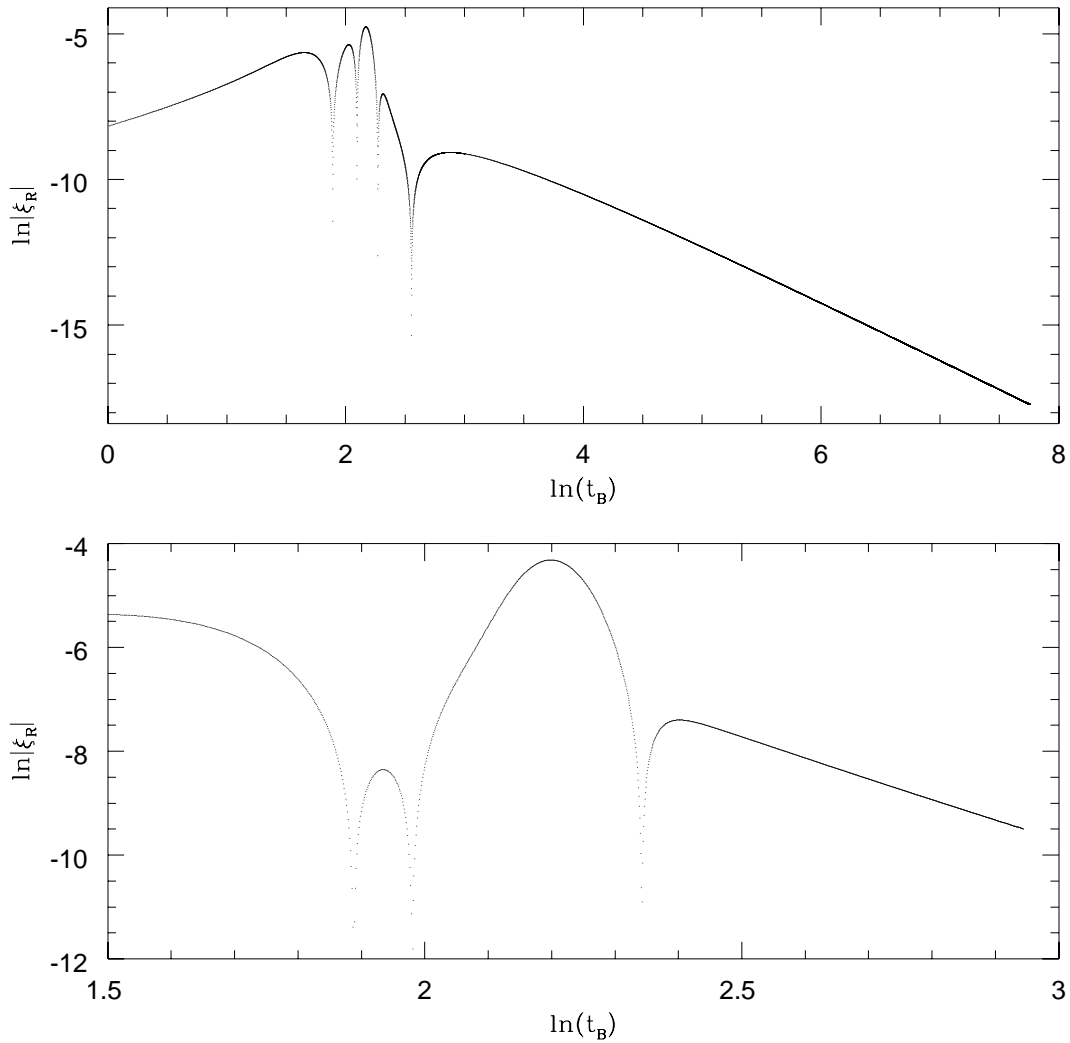


FIG. 4. Evolution of the charged test field  $|\xi_R(r = 10, t)|$  on a *time-dependent* spacetime. The initial data for the background field  $\phi$  are those of Fig. 2. (*non-collapsing* case). The initial data for the test field  $\xi$  is a Gaussian distribution (multiplied by an  $r^2$  factor). A definite *power-law* fall-off is manifest at late-times. The power-law exponents are  $-1.99$  for the  $l=0$  mode (top panel) and  $-4.16$  for the  $l=1$  mode (bottom panel). These values are to be compared with the *analytically* predicted values of  $-2.0$  and  $-4.0$ , respectively.

TABLES

TABLE I. Dependence of the dumping exponents at timelike infinity  $i_+$  on  $eQ$

$e$	$Q_{BH}$	$2\beta + 2$	Nonlinear exponents
0.50	-0.241	-1.97	-1.99
0.70	-0.344	-1.88	-1.93
0.85	-0.420	-1.70	-1.78
0.90	-0.443	-1.60	-1.65